Essential Role of Histidine 20 in the Catalytic Mechanism of *Escherichia coli* Peptidyl-tRNA Hydrolase

Jonathan J. Goodall, Guo Jun Chen,[+] and Malcolm G. P. Page*

Basilea Pharmaceutica Ltd., Grenzacherstrasse 487, CH-4005 Basel, Switzerland

Received October 9, 2003; Revised Manuscript Received January 5, 2004

ABSTRACT: The peptidyl-tRNA hydrolase (Pth) enzyme plays an essential role in recycling tRNA from peptidyl-tRNA that has prematurely dissociated from the ribosome. In this study of *Escherichia coli* Pth, the critical role of histidine 20 was investigated by site-directed mutagenesis, stopped-flow kinetic measurements, and chemical modification. The histidine residue at position 20 is known to play an important role in the hydrolysis reaction, but stopped-flow fluorescence measurements showed that, although the His20Asn Pth mutant enzyme was unable to hydrolyze the substrate, the enzyme retained the ability to bind peptidyl-tRNA. Chemical modification of Pth with diethyl pyrocarbonate (DEPC) showed that a residue, with a pK_a value of 6.3, was essential for substrate hydrolysis and that the stoichiometry of inhibition was 0.70 ± 0.06 mol of DEPC/mol of enzyme, indicating that modification of only a single residue by DEPC was responsible for the loss of activity. Parallel chemical modification studies with the His20Asn and Asp93Asn mutant enzymes showed that this essential residue was His20. These studies indicate that histidine 20 acts as the catalytic base in the hydrolysis of peptidyl-tRNA by Pth.

The peptidyl-tRNA hydrolase (Pth)[1] enzyme has been demonstrated to serve an essential function in bacteria, crucial for cell viability (*1*−*3*). Its biological role is to recycle tRNA, by cleaving the ester bond between tRNA and the peptide of peptidyl-tRNA (*4*), for reuse by the cell after premature dissociation of peptidyl-tRNA from the ribosome (*5*, *6*). Premature dissociation of peptidyl-tRNA occurs naturally during protein expression but can be induced to occur at a very high level by several classes of antibiotics, e.g., lincosamides and macrolides, which is suspected to be a part of the mechanism by which they exert their antibacterial properties (*7*). Mutations that produce defective Pth in eubacteria are lethal to the bacterial cell but not the eukaryotic cell (*1*, *8*). For example, a mutation in a temperature-sensitive *Escherichia coli* has been mapped to a single point mutation, Gly101Asp, in the gene encoding for Pth (*2*). *E. coli* expressing this Pth mutant will grow normally in comparison to the wild-type enzyme at a permissive temperature of 30 °C but will stop growing when raised to the nonpermissive temperature of 42 °C (*9*). This lethal phenotype is due to either the buildup of peptidyl-tRNA, which is toxic to the cell (*9*), or to starvation of the cell for tRNA molecules vital for the translation of proteins (*10*). Whatever the mechanism, inhibition of Pth renders the cell nonviable and also leads to hypersensitivity to those antibiotics listed above that promote premature dissociation of peptidyl-tRNA (*11*). Pth enzymes are ubiquitous in nature and have been found in bacteria, eukaryotes, and most recently in the archae (*8*, *9*). The sequence conservation of the Pth enzymes is particularly high between the known eubacterial genes. In addition, the mechanism of action of these bacterial enzymes has been demonstrated to be completely different to that of the rabbit reticulocyte Pth, which is the only mammalian enzyme characterized so far (*12*). Hence, Pth is of great interest as a target for antimicrobial agents, because a specific inhibitor of this enzyme would have a specific antibacterial activity. Despite this, very little biochemical information has been revealed about this enzyme. The structure of the *E. coli* enzyme has been solved to the 1.2-Å resolution (*13*), but so far, no structures showing enzyme−substrate interactions have been elucidated. However, the position of the active site has been proposed, based on the fortuitous binding of the C terminus of an adjacent Pth enzyme (*13*). Perhaps the major contributing factors to the lack of progress in the characterization of this enzyme have been the complete lack of any inhibitors of this enzyme and the reliance on radiolabeled substrates for assaying the activity. Recent advances in fluorescent subtrates have improved the ease with which this enzyme can be studied and will hopefully lead to the discovery of inhibitors of this enzyme, which can be used as the basis for antibiotics (*14*, *15*).

We report the inactivation of Pth by diethyl pyrocarbonate (DEPC), which supports the hypothesis that the catalytic mechanism of Pth involves a histidine residue in the cleavage of the ester bond of peptidyl-tRNA (*13*). This inactivation is stoichiometric and both time- and pH-dependent. The pK_a of the essential residue, identified as His20, has been determined to be 6.3. The proposed active site of Pth has been defined around His20, from crystallographic data (*13*), and these data showed that this residue is ideally placed for

* To whom correspondence should be addressed. Tel: (+41) 616061399. Fax: (+41) 616061112. E-mail: malcolm.page@basileapharma.com.

[+] Current address: F. Hoffmann-La Roche AG, CH-4070 Basel, Switzerland.

[1] Abbreviations: Pth, peptidyl-tRNA hydrolase; $tRNA^{Met}$, methionine-specific transfer RNA; DEPC, diethyl pyrocarbonate; GST, glutathione S transferase.

10.1021/bi0302200 CCC: $27.50
Published on Web 03/26/2004

an important role in catalysis by this enzyme. Chemical modification and mutagenesis experiments have demonstrated that this residue is essential for the catalytic activity of the enzyme, but transient-state kinetic experiments have also clearly shown that the mutant His20Asn retains the ability to bind the substrate (*15*). Thus, it appears that residue histidine 20 acts as the catalytic base in the mechanism of the enzyme, to activate a hydrolytic water molecule orientated to attack the ester carbonyl bond between tRNA and the peptidyl portions of peptidyl-tRNA.

EXPERIMENTAL PROCEDURES

Materials. DEPC and picrylsulfonic acid were bought from Sigma. Oregon Green 488-X succinimidyl ester and Sytox Blue nucleic acid stain were purchased from Molecular Probes.

Cloning, Expression, and Purification of the Glutathione S Transferase Fused Pth Mutants. Mutant Pth enzymes were produced by introducing point mutations into the Pth sequence using Quick Change (Stratagene) site-directed mutagenesis (*15*, *16*). The same procedure, using appropriate oligonucleotides, was used to make point mutations at Asn10 (replaced by Asp), His20 (replaced by Asn, Gln), Met67 (replaced by Glu), Asp93 (replaced by Asn), Lys103 (replaced by Arg, Glu, Ser), Lys105 (replaced by Arg, Glu, Ser), and His113 (replaced by Gln). The coding region of Pth was inserted into the pGEX-4T-3 plasmid (Amersham Biosciences) between the restriction sites *Bam*HI and *Sal*I to produce a glutathione S transferase (GST) fused Pth enzyme, expressed under the control of the lac promoter and inducible with isopropyl-β-D-thiogalactopyranoside (IPTG) (*16*). The GST-Pth fusion enzymes were then expressed in *E. coli* Sure 2 cells and purified using glutathione-sepharose 4B (Pharmacia). For purification, bacteria harboring the appropriate plasmid were grown at 37 °C in Luria Broth, containing 100 mg L^{-1} ampicillin, to an optical density at 600 nm of 0.5−0.8. IPTG was added to a final concentration of 0.5 mM, and the incubation continued for another 2−3 h with shaking. The cells were collected by centrifugation at 5000*g* for 15 min. Typically, 5 L of the culture produced 3−6 g of wet weight of the cell pellet. The cell pellet from the 1 L culture was suspended in 5 mL of ice cold 50 mM Tris adjusted to pH 7.5 with 4 M HCl, containing 150 mM NaCl, 1 mM Na EDTA, and 10 mM β-mercaptoethanol. Cells were disrupted on ice using a Heat Systems-Ultasonics Inc. W-375 sonicator equipped with a microtip and set for 50% output for 120 pulses. The cell debris was removed by centrifugation at 20 000*g* for 45 min. The supernatant was then mixed with 1 mL of the 50% (v/v) glutathione agarose slurry in the disruption buffer and incubated on ice for 1 h with intermittent shaking. The mixture was transferred to a 1 mL disposable column (Qiagen), and the resin was transferred with 3 × 1 mL of disruption buffer and then with 5 × 1 mL of the same buffer but with 500 mL of NaCl and then once with 1 mL of 50 mM Tris adjusted to pH 8.0 with 4 M HCl, containing 150 mM NaCl, 1 mM Na EDTA, and 10 mM β-mercaptoethanol. The GST-fusion proteins were then eluted with 4 mL of 50 mM Tris adjusted to pH 8.0 with 4 M HCl, containing 150 mM NaCl, 1 mM Na EDTA, 10 mM β-mercaptoethanol, and 10 mM reduced glutathione. The protein was concentrated using Eppendorf centrifugal filter tubes with a molecular weight cutoff of 10 000 Da. The GST-Pth-fusion protein was the only band to be seen by Coomassie Blue staining of 15% polyacrylamide gels after electrophoresis. The purified GST-fusion proteins were stored in 50 mM Tris-HCl, 1 mM EDTA, and 10 mM β-mercaptoethanol, and the protein concentrations were determined using the Micro BCA (Pierce) protein determination kit. These mutant Pth enzymes were used as the GST-fusion proteins in both the steady-state and stopped-flow kinetic measurements.

Purification of Wild-Type E. coli Pth and the His20Asn and Asp93Asn Mutants. Wild-type *E. coli* Pth enzyme and the Pth mutant enzymes, free from GST fusion, were purified from a culture of IPTG-induced *E. coli* Sure 2 cells harboring the appropriate Pth overexpression plasmid (*16*), with only a slight modification from the method of Kössel (*6*). The bacteria were grown, and the Pth expression was induced as described above for the GST-fusion proteins. About 35 g of the wet-cell paste was suspended in 35 mL of ice-cold 100 mM Tris, adjusted to pH 7.5, containing 1 mM Na EDTA and 10 mM β-mercaptoethanol, and the cells were disrupted by passage twice through a French press at 10 000 psi. The cell debris was removed by centrifugation at 30 000*g* for 30 min at 4 °C, and the supernatant was partially purified by ammonium sulfate fractionation. The 35−75% fraction precipitate was collected by centrifugation at 30 000*g* for 30 min at 4 °C, dissolved in the minimum volume of 50 mM *N*-2-hydroxyethylpiperazine-*N*′-2-ethanesulfonic acid (HEPES) at pH 8.0, containing 0.1 mM Na EDTA and 10 mM β-mercaptoethanol, and then dialyzed against 2 L of the same buffer for 17 h with one buffer change. About 50 mL of dialysate was passed through a 0.22 μm low-protein-binding filter and applied to an 80 mL BioRad MicroPrep High Q column (26 × 150 mm) that was equilibrated in the same buffer. At this pH, Pth appeared in the flow through fraction, while most other proteins were absorbed onto the resin. The flow through fraction was loaded directly onto a 20 mL BioRad MicroPrep High S column (16 × 100 mm) equilibrated in the same buffer. The column was washed with the same buffer until the OD_{260} returned to the baseline. Pth was then eluted with a linear gradient, over 10 column volumes, of 0−300 mM NaCl in the same buffer. The enzyme eluted in the fractions between 130 and 160 mM NaCl. The protein gave a single band, estimated to be at least 98% pure. The purified GST-fusion proteins were stored in 50 mM Tris-HCl, 10 mM $MgCl_2$, 0.5 mM EDTA, and 10 mM β-mercaptoethanol, and the protein concentrations were determined using the Micro BCA (Pierce) protein determination kit.

Cloning, Expression, and Purification of $tRNA^{Met}m$ and Preparation of the Substrate for Pth Assay. Methionine-specific transfer RNA ($tRNA^{Met}$)m was isolated from *E. coli* cells containing a $tRNA^{Met}m$ expression plasmid, which was constructed by insertion of the *$tRNA^{Met}m$* gene into the pDS56/RBSII plasmid (*17*) between the *Eco*RI and *Sal*I sites (*16*), by phenol extraction. An acid phenol mixture (25:24:1 by volume of phenol/chloroform/isoamyl alcohol at pH 4.7) was used to give good separation from the protein and DNA (*18*, *19*). $tRNA^{Met}m$ was further purified on the BioRad Micro-Prep (diethylamino)ethyl (DEAE) column following the reported procedure (*20*). The charging with methionine was carried out at room temperature in a reaction mixture

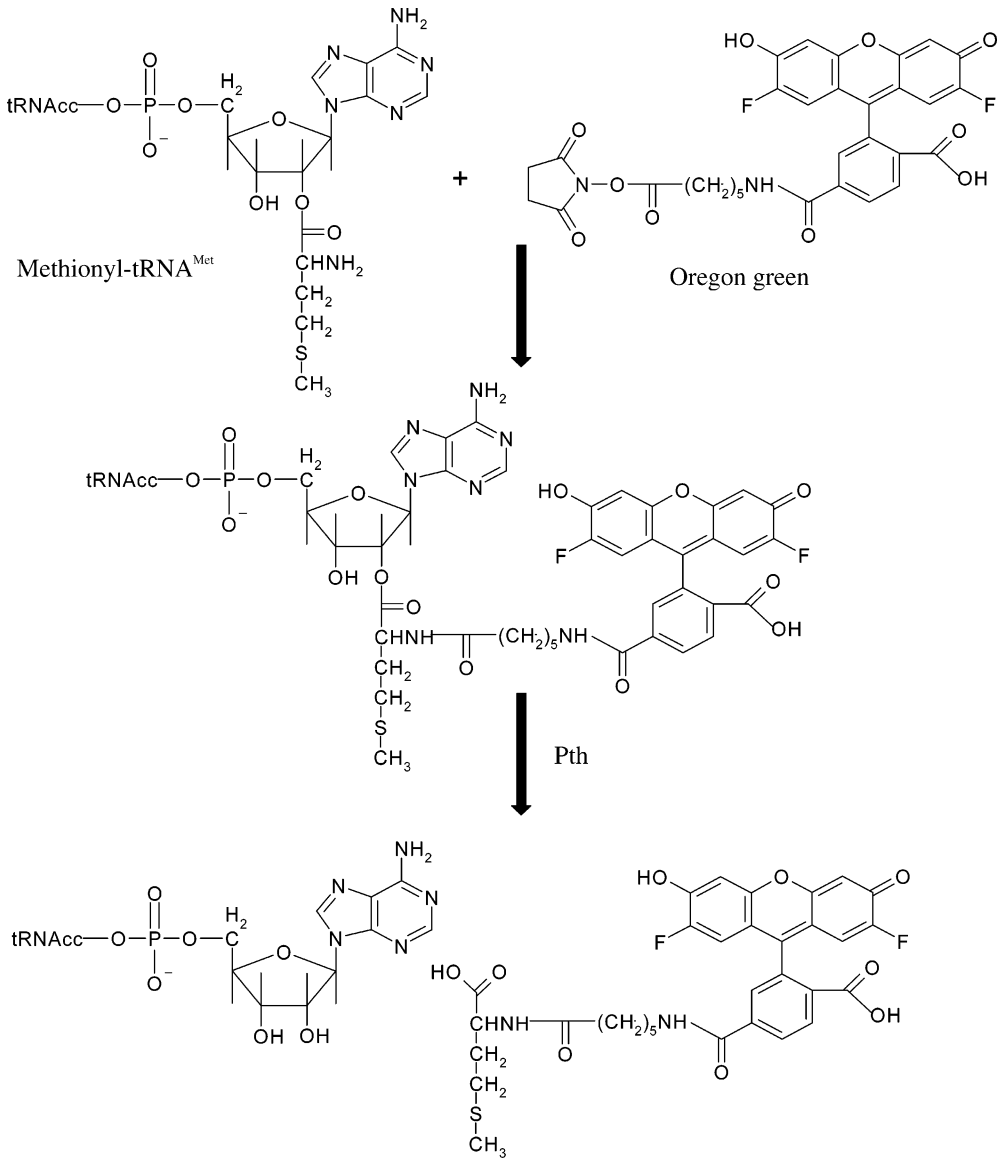

FIGURE 1: Synthesis and enzymatic hydrolysis of Oregon Green methionine tRNA^{Met} substrate for bacterial Pth.

containing 50 mM HEPES, adjusted to pH 7.4 with 5 M KOH, 15 mM magnesium acetate, 15 mM dithiothreitol (DTT), 100 mM KCl, 5 mM ATP, 10 mM L-methionine, 50 nM *E. coli* methionyl-tRNA synthetase (*16*), and 200 OD_{260} units of partially purified tRNA^{Met}m (*21*). After incubation for 30 min, the reaction mixture was separated by DEAE chromatography, as described above, and the recovered tRNA was used for labeling without further characterization. Labeling was conducted in 1 mL of a 0.5 M citric acid buffer, adjusted to pH 6.0 with KOH, containing 1.5 mg of Oregon Green 488-X carboxylic acid succinimidyl ester (Molecular Probes) and 100 OD_{260} units of methionyl-tRNA^{Met}m. After incubation for 4 h at room temperature, the labeled methionyl-tRNA^{Met}m was purified using a 25 mL BioRad Macro-Prep DEAE column (10 × 300 mm) with a linear NaCl gradient from 550 to 800 mM in a 25 mM sodium phosphate buffer at pH 6.0, containing 0.5 mM Na EDTA. The fractions containing the substrate were pooled, lyophilized, and stored in an 80% ethanol solution at −20 °C. Before use, the substrate suspension was centrifuged and the pellet dissolved in the reaction buffer. The purified substrate could be cleaved to >95% by Pth, and only a peak corresponding to Oregon-Green-labeled methionine was identified by mass spectroscopy of the hydrolysis mixture. The substrate had an OD_{260}/OD_{495} ratio of 8 ± 0.5, which corresponds to a molar ratio of tRNA to Oregon Green 488-X of approximately 1.

Pth Activity Assay. The activity of Pth was measured using a new fluorescence assay (Figure 1). The substrate used for these measurements was produced by a procedure similar to that used by Bonin and Erickson (*14*), but tRNA^{lys} was replaced by tRNA^{met} and the dye used for labeling was Oregon Green 488-X succinimidyl ester (Molecular Probes) rather than Bodipy succinimidyl ester. This fluorescent substrate was then modified for use in a continuous activity assay by the addition of a 2-fold excess of Sytox Blue nucleic acid stain (Figure 2). Before cleavage of the substrate, the emission spectrum of the Sytox Blue dye is quenched because of its proximity to the Oregon Green dye of the substrate, whose excitation spectrum overlaps the emission spectrum of Sytox Blue. After cleavage of the substrate, the distance between the Sytox Blue dye and the Oregon Green dye increases with a resultant release of quenching. This effect allows the hydrolysis of the substrate to be followed

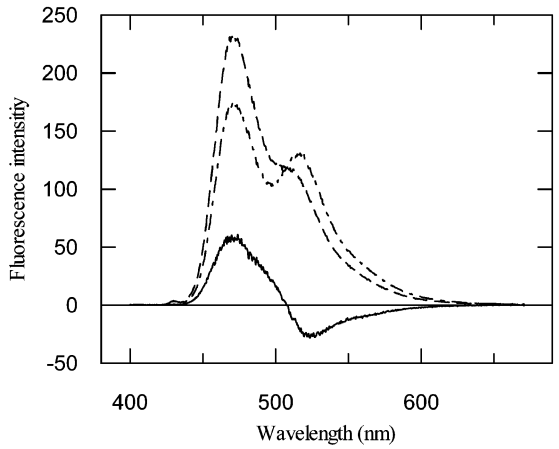

FIGURE 2: Fluorescence change upon hydrolysis of Oregon Green tRNA Sytox Blue substrate. Fluorescence spectra shown represent the modified substrate before addition of the enzyme (dash-dotted line), after addition of the enzyme (dashed line), and the difference (solid line), upon excitation at 430 nm. The reaction conditions were a final reaction volume of 50 μL, Oregon Green tRNA substrate concentration of 10 μM, and Sytox Blue concentration of 20 μM, and the reaction was taken to completion by the addition of *E. coli* Pth to a final concentration of 20 μM.

and provides an extremely sensitive and continuous assay of Pth activity.

To assay the enzymatic activity of Pth, 20 μL of the filtered substrate in 50 mM Tris-HCl, 10 mM $MgCl_2$, 0.5 mM EDTA, and 2 mM β-mercaptoethanol at pH 7.5 was pipetted per well into a 384 well plate and the enzyme was added to a final concentration of 10 nM. Rates were measured at room temperature by fluorescence spectroscopy on an Analyst AD plate reader from LJL Biosystems, fitted with a 425 nm excitation filter (35 nm) and 480 nm emission filter (10−25 nm).

Steady-State Kinetic Measurements. The continuous fluorometric assay described above was used for the determination of the Michaelis−Menten parameters of both the Pth enzyme and Pth mutant enzymes, and the K_m and k_{cat} values were determined by fitting the data to the Michaelis−Menten equation using the Grafit software package (Erithacus Software Ltd.).

Transient-State Kinetic Analysis by Stopped-Flow Fluorescence. Stopped-flow fluorescence measurements were carried out on a model SF-61 DX2 stopped-flow apparatus (Hi-Tech Scientific). Binding was monitored by following the increase in fluorescence emission at 535 nm concomitant with the binding when the Pth substrate was excited at 508 nm. All stopped-flow experiments were carried out under single turnover conditions of the excess enzyme in 50 mM Tris-HCl at pH 7.5, 10 mM $MgCl_2$, 0.5 mM EDTA, and 2 mM β-mercaptoethanol at 25 °C. Data were then fitted to eq 1 where k_b is the observed rate of binding, k_1, the rate

$$k_b = k_1[E] + (k_{-1} + k_2) \quad (1)$$

constant for association, [E], the enzyme concentration, k_{-1}, the rate constant for dissociation, and k_2, the rate of hydrolysis.

Chemical Modification of Pth with DEPC. DEPC was used to investigate the importance of histidine residues in the catalytic mechanism. To inhibit Pth with DEPC, 2 μM *E. coli* Pth was incubated with various concentrations of DEPC from 0.005 to 0.5 mM in a volume of 200 μL in 50 mM MOPS−KOH at pH 7.0. The concentration of DEPC was determined by the method of Miles (*22*) and stored in dry MeCN. At 0, 1, 2, 4, 6, 8, and 10 min time intervals, 10 μL aliquots were taken and the reaction was quenched by diluting it 10-fold into the reaction buffer containing 100 mM L-histidine. To determine the residual activity of the enzyme, after reaction with DEPC, the activity was assayed using the modified Pth assay in the plate format described above. The apparent rate constant for the rate of inhibition of the Pth enzyme by DEPC was calculated from a first-order exponential plot of (A_t/A_0) versus time, where A_0 is the activity of Pth before addition of DEPC and A_t is the activity at each time point. The order of the inactivation reaction was calculated from a logarithmic plot of k_{obs} versus DEPC concentration by fitting it to eq 2 where k_{obs} is the

$$\log k_{obs} = n \log [DEPC] + \log k_{ac}^{h} \quad (2)$$

apparent rate constant of inactivation, k_{ac}^{h} is the second-order rate constant for carbethoxylation at a fixed pH, [DEPC] is the concentration of DEPC, and n is the order of the reaction.

The pK_a of the group modified by DEPC was determined by measuring the apparent rate constant for inactivation of Pth by DEPC in a 50 mM MOPS−KOH buffer at various pH values between 6.3 and 7.5, with the concentration of DEPC kept constant at 0.05 mM. The assay was carried out as described above with the aliquots removed at the various time intervals and the apparent rate constant of inactivation being determined from the first-order exponential plot of (A_t/A_0) versus time. The rate of inactivation k_{obs} of Pth by DEPC is dependent on the modification of a residue in its basic form; it is dependent on the ionization constant and pH according to eq 3 where k_{ac}^{h} is the pH-independent rate

$$k_{obs} = \frac{k_{ac}^{h} K_a}{K_a + [H^+]} \quad (3)$$

constant for carbethoxylation at a particular DEPC concentration, K_a is the apparent ionization constant, and $[H^+]$ is the hydrogen ion concentration (*23*).

The rate of inactivation of Pth by DEPC is linear with the DEPC concentration, and therefore eq 3 can be rearranged into the form

$$\frac{k_{obs}}{[DEPC]} = \frac{k_{ac}^{h}}{[DEPC]} - \left(\left(\frac{k_{obs}[H^+]}{K_a}\right)\frac{1}{[DEPC]}\right)$$

This form allows a linear plot whereby the pK_a of the group inactivated by DEPC can be calculated from the slope of the resulting straight line and the pH-independent rate of inactivation can be determined from the intercept on the abscissa.

Spectrophotometric Measurement of the pK_a for the Reaction of DEPC with Wild-Type Pth, Asp93Asn, and Imidazole. The rate of reaction between 1 mM DEPC and either Pth, Asp93Asn mutant Pth, or imidazole, all at a 50 μM concentration, was measured by fitting the increase in absorbance at 240 nm upon reaction with DEPC as a function of time to a first-order exponential equation. The resulting

Table 1: Steady-State Kinetic Parameters of the Pth Mutant Enzymes[a]

GST Pth	k_{cat} (s^{-1})	K_m (μM)	k_{cat}/K_m (μM^{-1} s^{-1})
wild type	9.3	5.5	1.7
Asn10Asp	0.005	7.9	0.0006
His20Asn	nd[b]	nd[b]	$<10^{-6}$
His20Gln	nd[b]	nd[b]	$<10^{-6}$
Met67Glu	0.045	3.6	0.013
Asp93Asn	0.37	3.8	0.1
Lys103Arg	6.3	4.1	1.5
Lys103Gln	5	23	0.22
Lys103Ser	2.6	37	0.07
Lys105Arg	2.4	8.7	0.28
Lys105Gln	1.9	36	0.053
Lys105Ser	1.5	30	0.05
His113Gln	9.1	24	0.38

[a] The error in all cases was no greater than 10%. [b] Not determinable (rate of substrate hydrolysis was below the limit of detection).

rate and pH data were then fitted to eq 4 to calculate the pK_a values for the modified residues.

When the reaction of interest was of a chemical nature and not enzymatic, which was the case with reactions between Pth and DEPC, the full-length mutant enzymes were used in experiments, because the contribution to the observed reaction from the wild-type contamination would be negligible.

Treatment of DEPC-Modified Pth with Hydroxylamine. The Pth enzyme (2 μM) was reacted with 0.5 mM DEPC in 50 mM HEPES−KOH at pH 7.0 and incubated at 25 °C for 10 min to completely inactivate the enzyme. Then, an aliquot from this reaction was diluted 10-fold into a solution of 50 mM HEPES−KOH at pH 7.0 and 100 mM L-histidine, either containing 200 mM hydroxylamine or without hydroxylamine. The excess histidine was added to the solution to quench any further reaction of DEPC with histidine residues on the enzyme. After 6 h of treatment with or without hydroxylamine, the activity of these samples and of the control to which no DEPC had been added was assayed.

RESULTS

Steady-State Kinetic Parameters of Pth and Pth Mutant Enzymes. The results of the mutational studies on Pth are shown in Table 1. It was not possible to obtain kinetic parameters for the hydrolysis reaction of mutants of residue His20 because their residual activity was below the level of detection ($k_{cat}/K_m < 10^{-6}$ μM^{-1} s^{-1}), demonstrating that it is likely that there is an important role for this residue in the hydrolysis reaction of Pth. Another residue, Asp93 was also identified as having an important role, because a mutation of this Asp residue to an Asn leads to a significant effect (25-fold decrease) on the k_{cat} of the enzyme.

These studies highlighted a number of other residues that also appear to play an important role in catalysis. Both Asn10 and Met67 had a key role, because a change to another amino acid in these positions caused a marked loss in activity, with a greater than 200-fold decrease in the k_{cat} value. The positive charge on residues Lys103 and Lys105 was shown to be important, and a change to a neutral residue in any of these positions led to an increase in the K_m values; however, substitution with another positively charged side chain had a minimal effect. This may suggest a role in binding of the strongly negatively charged tRNA portion of the substrate (*24*).

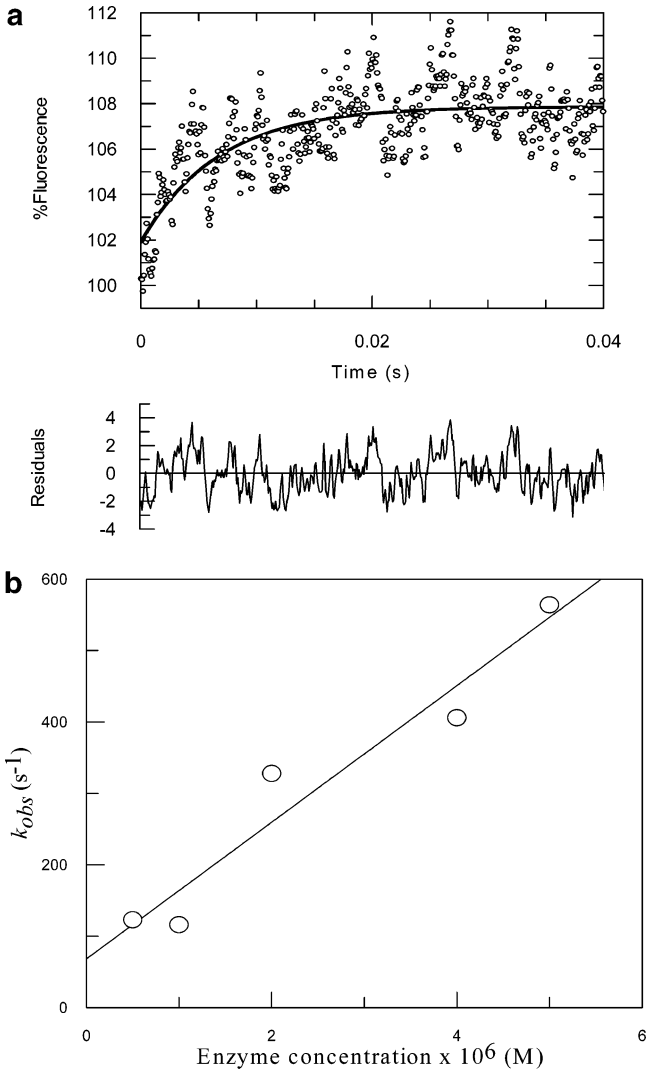

FIGURE 3: (a) Example of a stopped-flow trace obtained with the GST-fused His20Asn mutant in which equal volumes of the enzyme and substrate solution were mixed to a final concentration of 10 μM and 0.05 μM, respectively. The observed rate of binding k_{obs} was determined by fitting the increase in fluorescence at 532 nm upon excitation at 508 nm by a first-order exponential. Fluorescence values are given as a percentage of the premixing fluorescence. (b) Concentration dependence of binding of Oregon Green methionine $tRNA^{met}$ to a GST-fused His20Asn mutant of *E. coli* Pth under conditions of an excess enzyme.

Binding of the Fluorescent Substrate to the His20Asn Mutant Pth. The Pth assay without addition of Sytox Blue was used to observe whether the Pth mutant His20Asn was still able to bind the substrate. Upon binding, there is an increase in the fluorescence signal from the substrate that was observed by stopped-flow fluorescence spectroscopy (Figure 3a). The observed rate constant for the binding of the Pth substrate to the His20Asn mutant was plotted against the concentration of the substrate (Figure 3b), allowing both the rate constant for the association and the rate constant for the dissociation to be calculated. The value calculated for the rate constant of association is $95 \pm 8 \times 10^6$ M^{-1} s^{-1}, and the rate constant for dissociation was calculated as 68 $\pm$ 6 s^{-1}.

Inhibition Kinetics of Pth by DEPC. Inactivation of Pth by DEPC has been demonstrated, supporting the idea that a

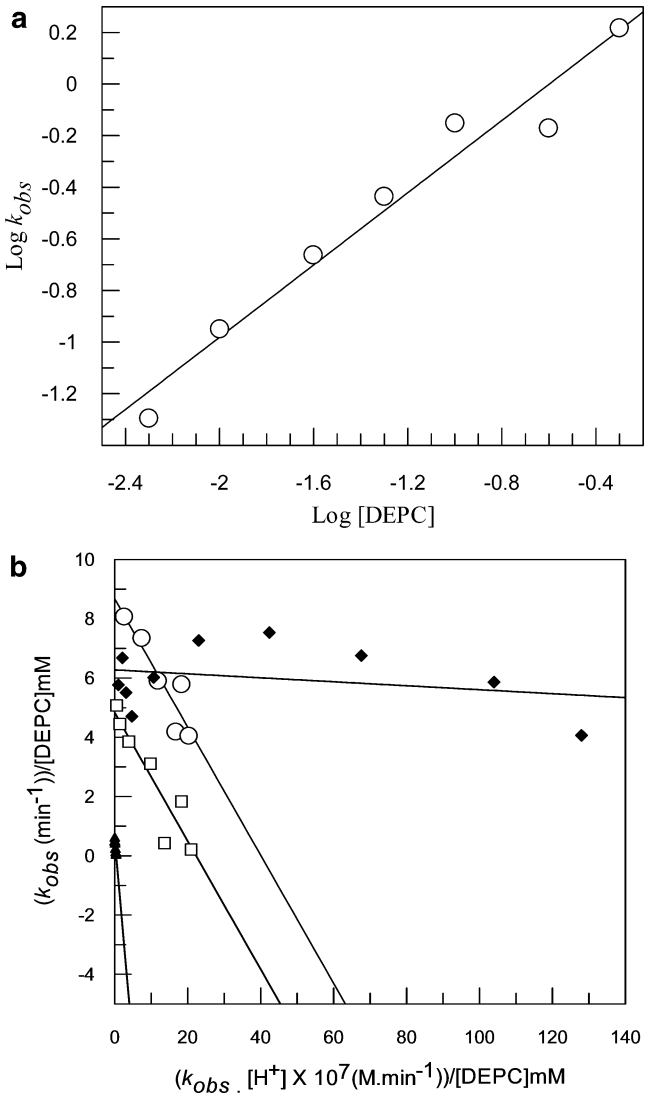

FIGURE 4: (a) Plot of the logarithm of the observed rate of inactivation of Pth by DEPC versus the logarithm of the DEPC concentration (millimolar). The points were fitted to eq 2. From the plot, a value for the second-order rate constant for acylation at a fixed pH (k_{ac}^{h}) of $(2.63 \pm 1.23) \times 10^{-3}$ M^{-1} min^{-1} and a reaction order of 0.70 ± 0.06 was derived. (b) pH dependence of the reaction of DEPC with both wild-type Pth enzyme and imidazole. Data displayed as open circles are the reaction of DEPC within wild-type Pth measured by inactivation, whereas the data displayed as open squares, filled triangles, and filled diamonds relate to the direct spectrophotometric observation of the reaction between wild-type Pth, imidazole, and Asp93Asn, respectively.

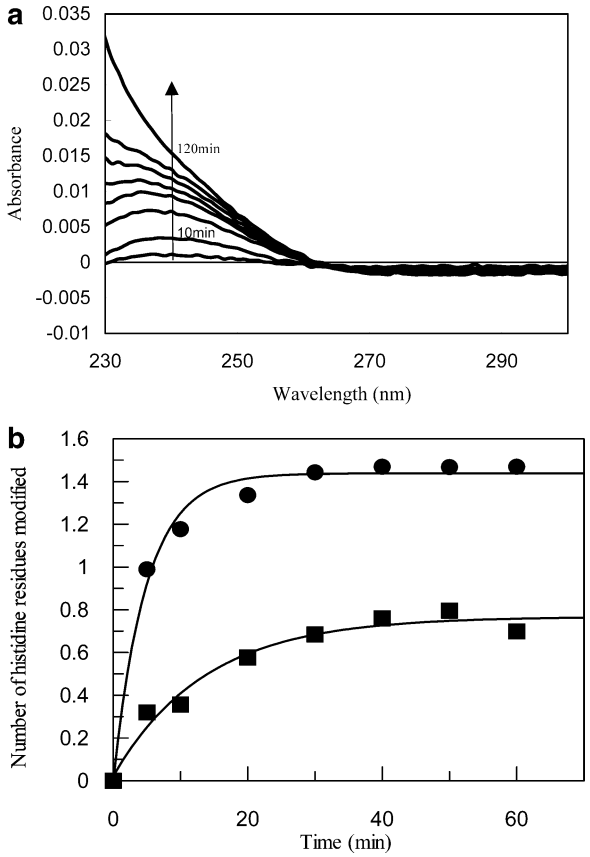

FIGURE 5: (a) Difference spectrum showing the increase in absorbance caused by the formation of carbethoxyhistidine upon the addition of 0.1 mM DEPC to 2 μM Pth in 50 mM MOPS−KOH at pH 7.0. The spectra were recorded after 5, 10, 20, 30, 40, 50, 60, and 120 min of incubation. (b) Labeling of histidine residues in wild-type Pth (circles) and His20Asn Pth (squares) as a function of time when 0.5 mM DEPC was added to 2 μM Pth in 50 mM HEPES−KOH at pH 7.0. The number of histidines labeled was calculated from the UV absorbance at 240 nm, assuming an extinction coefficient at 240 nm of 3200 M^{-1} cm^{-1} (*35*).

histidine residue is involved in the cleavage of the ester bond of peptidyl-tRNA by Pth (*13*). The order of the reaction resulting in inhibition of Pth by diethyl pyrocarbonate was determined from the slope of a plot of the logarithm of the observed rate of DEPC inhibition versus the logarithm of the DEPC concentration (*25*). This gave a value of 0.70 ± 0.06 (Figure 4a), suggesting that the reaction with one site on Pth is sufficient to completely inhibit of the enzyme.

Further evidence to support the stoichiometry of the reaction between DEPC and Pth was obtained from direct spectrophotometric measurements. Modification of a histidine residue, forming a carbethoxyhistidine, can be observed by a change in the ultraviolet spectrum at 240 nm. Different spectra collected in the region of 220−320 nm (Figure 5a) clearly demonstrated that there was a time-dependent increase in absorbance attributable to the formation of a carbethoxyhistidine group. Upon modification by 0.5 mM DEPC, the activity of the 2 μM Pth enzyme was decreased in less than 10 min by greater than 90%. Changes in the ultraviolet spectrum, under the same conditions, suggested that after this time approximately 1.2 mol of DEPC/mol of enzyme had reacted (Figure 5b). Hence, it can be concluded that inactivation of the Pth enzyme relates to the modification of a single histidine residue. Further, when an exhaustive labeling experiment was carried out on the His20Asn mutant Pth enzyme and on the wild type, after 1 h, only 0.7 mol of DEPC/mol of enzyme reacted with the mutant compared to 1.5 mol of DEPC/mol of enzyme in the reaction with the wild type. The difference, approximately 0.8 mol of DEPC/mol of enzyme, is attributable to the absence of His20.

Recovery of the Pth Activity, after DEPC Modification, by Treatment with Hydroxylamine. It has been shown that, of the residues modified by DEPC, only histidine and tyrosine can be regenerated from the treatment with hydroxylamine (*26*). The activity of the DEPC-modified Pth recovered approximately 41% of the activity of the control enzyme that had not been modified with DEPC after the treatment with 200 mM hydroxylamine, whereas the DEPC-

Table 2: pH-Independent Inactivation Rate for Carbethoxylation (k_{ac}) and pK_a Data for Wild-Type Pth, Asp93Asn Mutant Pth, and Imidazole[a]

E. coli Pth enzyme	k_{ac} (min^{-1}/[DEPC]mM)	pK_a
wild type (inactivation)	8.67 ± 0.67	6.3 ± 0.1
wild type (direct)	4.83 ± 0.50	6.3 ± 0.1
Asp93Asn	6.27 ± 0.47	4.8 ± 0.3
imidazole	0.53 ± 0.02	7.1 ± 0.1

[a] Values determined from the linear plot (eq 4).

modified enzyme that had not been treated with hydroxylamine recovered less than 1% of the activity of the control (data not shown). Hence, the modification of Pth by DEPC is at least partially reversible from the treatment with hydroxylamine. This makes it unlikely that a residue other than tyrosine or histidine is the residue modified by DEPC leading to inactivation of Pth. In the spectrophotometric assay for DEPC modification, there was no observable change in the spectrum at 280 nm, characteristic of a reaction with tyrosine, suggesting that the diethyl pyrocarbonate modification had not altered any of the tyrosine residues in the protein.

pH Dependence of DEPC Inhibition. The pH dependence of inactivation of Pth was fitted to eq 4 to estimate the pK_a of the residues modified by DEPC. The pK_a value obtained for the reaction of DEPC with wild-type Pth by this method was 6.3 ± 0.1 (Figure 4b).

The increase in absorbance at 240 nm was used to directly determine the pH dependence of the reaction of DEPC with imidazole and with both wild-type and Asp93Asn mutant Pth enzymes. The pH-independent rate constant and pK_a value obtained for the modification of wild-type Pth were very similar to those determined in the inactivation experiment. This rate was considerably higher, and the pK_a was lower than those determined both for imidazole in an aqueous buffer and for the Asp93Asn mutant (Table 2).

DISCUSSION

The continuous fluorescence assay used in these experiments yielded kinetic parameters comparable to those published for the radiometric assay previously used to investigate this class of enzymes (*27*−*29*). The advantages of this fluorescence-based assay are its ease of use and ready detection of hydrolysis of the substrate. The addition of Sytox Blue, which intercalates with the double-stranded regions of the tRNA, did not alter the kinetic parameters of the enzyme for the substrate but has the advantage of allowing excitation and emission wavelengths to be selected that are more suitable for the application of the assay in a plate format. It was also found that this substrate was suitable for the measurement of the activity of the Pth enzyme from *Streptococcus pneumoniae* (*15*), demonstrating that the substrate is possibly broadly applicable to the assay of Pth enzyme activity from both Gram-positive and Gram-negative bacteria.

The active site of Pth has been proposed from the X-ray crystal structure to form a crevice surrounding residues His20, Asp93, and His113. Extensive site-directed mutagenesis studies have been used to identify many of the important residues involved in the binding of the substrate and in the catalytic mechanism of this enzyme (*13*, *14*). From these mutagenesis studies, it has been proposed that binding of the strongly negatively charged tRNA portion of peptidyl-tRNA requires the involvement of a number of cationic regions and several of these have been identified. For example, both the region centered around Arg133, where a mutation to a histidine residue is responsible for the Pth (rap) phenotype, which was identified by its inability to support vegetative growth of bacteriophage λ (*2*, *30*), and the region around Lys142, whose side chain protrudes out into the cleft of the presumed active site, have been demonstrated to be important in the binding of the substrate (*13*). There are also residues, further away from the proposed active site, where the contribution of their positive charge appears to have an important role in the activity of the Pth enzyme, notably, the lysine residues Lys103 and Lys105 (Table 1), where a change to a neutral amino acid causes a significant increase in the K_m value. However, there was no significant effect on the K_m upon substitution of these residues with a positively charged amino acid such as arginine, despite the fact that their side chains do not appear from the X-ray structure to form salt bridges. These residues are adjacent to residue Gly100 that upon mutation to asparagine is responsible for the temperature-sensitive phenotype of Pth (*2*) and is located on a section of β sheet that delineates the groove that runs along the Pth enzyme to the active site. Small changes in the orientation of these residues caused by a raise in temperature over the permissive temperature may hold the key to this phenotype.

Mutagenesis studies on residue His20 have shown that it is essential for the catalytic activity of the Pth enzyme, but transient kinetic experiments showed that mutants of this His20 residue retain the ability to bind the substrate. Hence, it is concluded that the role of the His20 residue is predominantly in the hydrolysis of peptidyl-tRNA and it is not essential to the binding of the substrate. The role of His20 in the catalytic mechanism was further probed by chemical modification of Pth by DEPC. These studies showed that the Pth enzyme was fully inactivated by modification of a single histidine residue and that this is most likely to be His20. The pH dependence of modification of Pth by DEPC, monitored by inactivation and spectrophotometry, showed that His20 has a pK_a value of 6.3, which is typical for the modification of a histidine residue (*26*). The pK_a value was lower, and the pH-independent rate constant for ethoxyformylation was higher than the respective values obtained with imidazole under similar conditions, which means that the His20 residue is a much better nucleophile than imidazole in an aqueous solution.

It is quite possible that the pK_a of His20 would be perturbed by formation of the enzyme−substrate complex, and thus, it cannot be assumed that the pH dependence of activity will reflect the pH dependence of the DEPC modification. The reported pH dependence of Pth activity shows that Pth hydrolysis of *N*-acylaminoacyl-tRNA has a plateau in the pH region 7−9, with the activity decreasing at pH values below 7 (*5*). This decrease in activity below pH 7 was interpreted as being caused by inactivation of either the enzyme or the substrate, but in view of the pK_a value determined by DEPC modification, it is likely that the decrease in activity at low pH is due to protonation of the enzyme−substrate complex. The pK_a value calculated for this enzyme−substrate complex is approximately 7.0, which

is higher than the pK_a value of 6.3 determined for DEPC labeling of Pth, indicating that the negative charge on the substrate shifts the pK_a by altering the microenvironment within the active site of the enzyme.

The active-site environment of Pth is likely to profoundly influence the ionization state of His20, and the position of Asp93 in the X-ray structure indicates a role for this residue in stabilizing the basic form of the histidine. Mutation of Asp93 to either asparagine (Table 1) or alanine (*13*) caused a considerable change in the k_{cat} of the enzyme but did not greatly change the K_m. The fact that Asp93 has a role in controlling the ionization state of His20 during catalysis was demonstrated by the pH dependence of the reaction between DEPC and an Asp93Asn mutant Pth. This clearly showed that in this mutant enzyme the pK_a value was shifted from 6.3 for the wild-type enzyme to 4.8 for the Asp93Asn mutant enzyme. The pH-independent rate of carbethoxylation was not significantly changed. The positive charge on His20 thus becomes markedly less stable after the interaction with Asp93 is perturbed. This suggests a role for Asp93 that is directly analogous to that of the aspartate residue in the charge-relay system of the serine proteinases (*31*), which has been demonstrated to be involved in both stabilizing the anionic form and orienting the catalytic base (*32*, *33*). The replacement of Asp93 by Asn causes the pK_a of His20 to fall by approximately 1.5 pH units, and assuming a β value for the attack of the substrate ester-carbonyl of 0.5 (*34*), the apparent second-order rate constant k_{cat}/K_m would be expected to be decreased by approximately 6.5-fold. In fact, the mutation of Asp93 to Asn leads to a 17-fold reduction of k_{cat}/K_m, suggesting that Asp93 also plays an important role in orienting His20 to accept a proton in its role as the catalytic base. This interaction between Asp93 and His20 is crucial to the mechanism used by Pth to hydrolyze the substrate and is analogous to the catalytic strategies used by many enzymes to tune their catalytic apparatus to meet their specific substrate requirements (*23*).

In conclusion, mutagenesis and chemical modification studies of Pth indicate that the extremely well-conserved His20 and Asp93 residues have an essential role in catalysis. This leads us to propose that hydrolysis of peptidyl-tRNA by Pth involves a mechanism whereby His20 is tuned to react with the ester bond of peptidyl-tRNA by a H bond between the Oγ of Asp93 and the N1 hydrogen of the His20 residue. This hydrogen bond stabilizes the anionic form of the histidine such that it will catalyze the hydrolysis of peptidyl-tRNA by accepting a proton from a proximal water molecule, which then in turn attacks the electrophilic carbon of the ester bond. This proposed mechanism requires confirmation by structural techniques such as X-ray crystallography, NMR, and neutron diffraction, which would allow the positioning of the residues involved in catalysis and their protons to be a accurately determined and solid conclusions about their role in catalysis to be drawn, or IR spectroscopy, which would help to identify intermediates in the reaction mechanism. As tools for studying Pth are developed and the mechanism by which it operates becomes elucidated in greater detail, the search for small molecule inhibitors of this target for use as possible novel antibiotics will be greatly eased, making the Pth enzymes an increasingly attractive topic for study.

ACKNOWLEDGMENT

The authors thank Na-Hong Qui for support and assistance during the course of this work and Dr. Franck Danel for helpful discussion.

REFERENCES

1. Menez, J., Buckingham, R. H., De Zamaroczy, M., and Campelli, C. K. (2002) Peptidyl-tRNA Hydrolase in *Bacillus subtilis*, Encoded by spoVC, is Essential to Vegetative Growth, Whereas the Homologous Enzyme in *Saccharomyces cerevisiae* is Dispenable. *Mol. Microbiol. 45*, 123−129.
2. Garcia-Villegas, M. R., De La Vega, F. M., Galindo, J. M., Segura, M., Buckingham, R. H., and Guarneros, G. (1991) Peptidyl-tRNA Hydrolase is Involved in Lambda Inhibition of Host Protein Synthesis. *EMBO J. 10*, 3549−3555.
3. Atherly, A. G., and Menninger, J. R. (1970) Mutant *E. coli* Strain with Temperature Sensitive Peptidyl-transfer RNA Hydrolase. *Nature, New Biol. 240*, 245−246.
4. Vogel, Z., Zamir, A., and Elson, D. (1968) On the Specificity and Stability of an Enzyme that Hydrolyzes N-Substituted Aminoacyl-transfer RNAs. *Proc. Natl. Acad. Sci. U.S.A. 61*, 701−707.
5. Kössel, H., and RajBhandary, V. L. (1968) Studies on Polynucleotides. LXXXVI. Enzymic Hydrolysis of N-acylamino-transfer RNA. *J. Mol. Biol.* 539−560.
6. Kössel, H. (1970) Purification and Properties of Peptidyl.tRNA Hydrolase from *Escherichia coli*. *Biochim. Biophys. Acta 204*, 191−202.
7. Menniger, J. R., and Otto, D. P. (1982) Erythromycin, Carbomycin and Spiramycin Inhibit Protein Synthesis by Stimulating the Dissociation of Peptidyl-tRNA from Ribosomes. *Antimicrob. Agents Chemother. 21*, 810−818.
8. Rosas-Sandoval, G., Ambrogelly, A., Rinehart, J., Wei, D., Cruz-Vera, L. R., Graham, D. E., Stetter, K. O., Guarneros, G., and Soll, D. (2002) Orthologs of a Novel Archaeal and of the Bacterial Peptidyl-tRNA Hydrolase are Nonessential in Yeast. *Proc. Natl. Acad. Sci. U.S.A. 99*, 16707−16712.
9. Menninger, J. R., Walker, C., and Tan, P. F. (1973) Studies on the Metabolic Role of Peptidyl-tRNA Hydrolase. I. Properties of a Mutant *E. coli* with Temperature-sensitive Peptidyl-tRNA hydrolase. *Mol. Gen. Genet. 121*, 307−324.
10. Heurgue-Hamard, V., Mora, L., Guarneros, G., and Buckingham, R. H. (1996) The Growth Defect in *Escherichia coli* Deficient in Peptidyl-tRNA Hydrolase is Due to Starvation for Lys-tRNA(Lys). *EMBO J. 15*, 2826−2833.
11. Menninger, J. R., and Coleman, R. A. (1993) Lincosamide Antibiotics Stimulate Dissociation of Peptidyl tRNA from Ribosomes. *Antimicrob. Agents Chemother. 37*, 2027−2029.
12. Gross, M., Crow, P., and White, J. (1992) The Site of Hydrolysis by Rabbit Reticulocyte Peptidyl-tRNA Hydrolase is the 3′-AMP Terminus of Susceptible tRNA Substrates. *J. Biol. Chem. 267*, 2080−2086.
13. Schmitt, E., Mechulam, Y., Fromant, M., Plateau, P., and Blanquet, S. (1997) Crystal Structure at 1.2 Å Resolution and Active Site Mapping of *Escherichia coli* Peptidyl tRNA Hydrolase. *EMBO J. 16*, 4760−4769.
14. Bonin, P. D., and Erickson, L. A. (2002) Development of a Fluorescence Polarization Assay for Peptidyl-tRNA Hydrolase. *Anal. Biochem. 306*, 8−16.
15. Chen, G. J. (2001) Investigation of the Reaction Mechanism of *E. coli* Peptidyl-tRNA hydrolase. Thesis, University of Basel, Basel, Switzerland.
16. Chen, G. J., Qiu, N., Karrer, C., Caspers, P., and Page, M. G. P. (2000) Restriction Site-Free Insertion of PCR Products Directionally into Vectors. *BioTechniques 28*, 498−5.
17. Stüber, D., Matile, H., and Garotta, G. (1990) System for High Level Production in *E. coli* and Rapid Purification of Recombinant Proteins: Application to Epitope Mapping, Preparation of Antibodies and Structure. Function Analysis. in *Immunological Methods* (Lefkovits, I., and Pernis, B., Eds.) Vol. IV, pp 121−152, Academic Press, Orlando, FL.
18. Chomczynski, P., and Sacchi, N. (1987) Single Step Method of RNA Isolation by Acid Guanidium Thiocyanate-Phenol-Chloroform Extraction. *Anal. Biochem. 162*, 156−159.

19. Puissant, C., and Houdebine, L. M. (1990) An Improvement of the Single-step Method of RNA Isolation by Acid Guanidium Thiocyanate-Phenol-Chloroform Extraction. *BioTechniques 8*, 148−149.
20. Nishimura, S., Harada, F., Narushima, U., and Seno, T. (1967) Purification of Methionine, Valine, Phenylalanine and Tyrosine Specific tRNA from *Escherichia coli*. *Biochim. Biophys. Acta 142*, 133−148.
21. Lawrence, F., Blanquet, S., Poiret M., Robert-Gero, M., and Waller, J. P. (1973) The Mechanism of Action of Methionyl tRNA Synthetase. 3. Ion Requirements and Kinetic Parameters of the ATP−PPi Exchange and Methionine Transfer Reactions Catalyzed by the Native and Trypsin-modified Enymes. *Eur. J. Biochem. 36*, 234−243.
22. Miles, E. W. (1977) Modification of Histidyl Residues in Proteins by Diethylpyrocarbonate. *Methods Enzymol. 47*, 431−442.
23. Fersht, A. (1985) *Enzyme Structure and Mechanism*, 2nd ed., W. H. Freeman and Company, New York.
24. Fromant, M., Plateau, P., Schmitt, E., Mechulam, Y., and Blanquet, S. (1999) Receptor Site for the 5′-Phosphate of Elongator tRNAs Governs Substrate Selection by Peptidyl tRNA Hydrolase. *Biochemistry 38*, 4982−4987.
25. Levy, H. M., Leber, P. D., and Ryan, E. M. (1963) Inactivation of Myosin by 2,4-dinitrophenol and Protection by Adenosine Triposphate and Other Phosphate Compounds. *J. Biol. Chem. 238*, 3654−3659.
26. Cousineau, J., and Meighen, E. (1976) Chemical Modification of Bacterial Luciferase with Ethoxyformic Anhydride: Evidence for an Essential Histidyl Residue. *Biochemistry 15*, 4992−5000.
27. Cuzin, F., Kretchmer, N., Greenberg, R. E., Hurwitz, R., and Chapeville, F. (1967) Enzymatic Hydrolysis of N-Substituted Aminoacyl tRNA. *Proc. Natl. Acad. Sci. U.S.A. 58*, 2079−2086.
28. de Groot, N., Panet, A., and Lapidot, Y. (1968) Enzymatic Hydrolysis of Peptidyl tRNA. *Biochem. Biophys. Res. Commun. 31*, 37−42.
29. Zucker, W. V. (1975) A New Method for Assaying Peptidyl-tRNA Hydrolase. *Anal. Biochem. 63*, 522−527.
30. Henderson, D., and Weil, J. A Mutant of *Escherichia coli* that Prevents Growth of Phage Lambda and is Bypassed by Lambda Mutants in a Non-essential Region of the Genome. (1976) *Virology 71*, 546−559.
31. Blow, D. M., Birktoft, J. J., and Hartley, B. S. (1969) Role of a Buried Acid Group in the Mechanism of Action of Chymotrypsin. *Nature 221*, 337−340.
32. Bryan, P., Pantoliano, M. W., Quill, S. G., Hsiao, H. Y., and Poulos, T. (1986) Site-directed Mutagenesis and the Role of the Oxyanion Hole in Subtilisin. *Proc. Natl. Acad. Sci. U.S.A. 83*, 3743−3745.
33. Fersht, A. R., and Sperling, J. (1973) The Charge Relay System in Chymotrypsin and Chymotrypsinogen. *J. Mol. Biol. 74*, 137−149.
34. Jencks, W. P., and Carriuolo, J. (1961) General Base Catalysis of Ester Hydrolysis. *J. Am. Chem. Soc. 83*, 1743−1750.
35. Chu, C. L., Hsiao, Y. Y., Chen, C. H., Van, R. C., Lin, W. J., and Pan, R. L. (2001) Inhibition of Plant Vacuolar H^+-ATPase by Diethylpyrocarbonate. *Biochim. Biophys. Acta 1506*, 12−22.

BI0302200